

Effects of Biopolymer Surfactants on the Morphology and Optical Properties of Zinc Sulphide (ZnS) Nanocrystalline Thin Film

Dorathy Awing Avit,¹ Suk-Fun Chin,^{1*} Noor Azie Azura Mohd Arif²
and Sahbudin Shaari³

¹Faculty of Resource Science and Technology, Universiti Malaysia Sarawak,
94300 Kota Samarahan, Sarawak, Malaysia

²Centre for Pre-University Studies, Universiti Malaysia Sarawak,
94300 Kota Samarahan, Sarawak, Malaysia

³Institute of Microengineering and Nanoelectronics, Universiti Kebangsaan Malaysia,
43600 Bangi, Selangor, Malaysia

*Corresponding author: sfchin@unimas.my

Published online: 25 November 2019

To cite this article: Avit, D. A. et al. (2019). Effects of biopolymer surfactants on the morphology and optical properties of zinc sulphide (ZnS) nanocrystalline thin film. *J. Phys. Sci.*, 30(3), 191–206, <https://doi.org/10.21315/jps2019.30.3.12>

To link to this article: <https://doi.org/10.21315/jps2019.30.3.12>

ABSTRACT: *Particle sizes of nanoparticles have significant effects on thin film properties such as the morphological and optical properties. However, controlling the size and morphology is a challenging task. One of the approaches towards overcoming these challenges is by using surfactants. This study reported the effects of several types of biopolymer surfactants on the size of zinc sulphide (ZnS) nanoparticles and the morphology of ZnS nanocrystalline thin films. The ZnS nanocrystalline thin films were fabricated by the spin-coating of ZnS nanoparticles on APTES [(3-aminopropyl) triethoxysilane] functionalised silica glass. Alginate acid, chitosan and starch were used as the surfactants to control the morphological and optical properties of the thin films. The XRD analysis confirmed the cubic structure and crystalline nature of the ZnS thin films. The field emission scanning electron microscope (FESEM) analysis revealed that the mean particle size of the ZnS nanocrystalline thin film to be within the range of 20–30 nm. The optical measurements revealed that all ZnS thin films exhibited a high transmittance of 92%–99% in the visible range. Photoluminescence (PL) spectra for all thin films were determined and exhibited their respective peaks at 470 nm and 620 nm.*

Keywords: Zinc sulphide, spin coating, biopolymer surfactant, nanocrystalline, thin film

1. INTRODUCTION

Zinc sulphide (ZnS) is a nontoxic II–VI compound semiconductor that has the novel properties of a wide direct band gap of 3.65–3.7 eV.¹ In view of its wide band gap value, ZnS thin films can be applied for the fabrication of optoelectronic devices, such as optical sensors, solar cells, anti-reflecting coatings and electroluminescent displays.^{2,3} The most significant feature of ZnS nanocrystal is their chemical and physical properties that differ greatly from those of their bulk counterparts. Due to ZnS' unique characteristics, many researchers have been interested to synthesise and study the properties of the its nanostructures. There are many methods available to synthesise ZnS nanoparticles, such as sol-gel, chemical precipitation method, inert gas condensation technique, ultrasonic radiation and hydrothermal process.^{4–8} Meanwhile, there are several different thin film deposition techniques such as spin coating, dip coating, chemical bath deposition, chemical spray pyrolysis and microwave irradiation.^{1,5,9–11}

One of the greatest challenges in synthesising nanoparticles is attaining a precise control for the nanoparticle size and the morphology of the resultant thin films, as most nanostructures will undergo aggregation and agglomeration.^{12,13} In recent years, tremendous efforts have been focused on using the surfactants like cetyltrimethylammonium bromide (CTAB), Triton x-100, cetyltrimethylammonium chloride (CTAC), polyvinylpyrrolidone (PVP), polyvinyl alcohol (PVA) and polyethylene glycol (PEG) for tailoring the morphology of the thin films. Such incorporation will also subsequently to fine-tune their optical properties for various specific applications.^{10,12–17} To the best of authors' knowledge, the use of biopolymers as the surfactant for the fabrication of ZnS thin films has not been explored extensively. Biopolymers are relatively low-cost, non-toxic, renewable and abundantly available, rendering them to be promising as surfactants for the fabrication of ZnS thin film.^{18,19} In this study, ZnS nanocrystalline thin films were fabricated by using the combined techniques of sol-gel and spin coating method. The effects of various biopolymer-based surfactant like starch, alginic acid and chitosan on the morphology and optical properties of the thin films were investigated.

2. EXPERIMENTAL

2.1 Materials and Reagents

Zinc acetate dihydrate (HmbG Chemicals) and Thiourea (Bendosen) were used as the precursors to synthesise ZnS nanoparticles (NPs). 3-Aminopropyl triethoxysilane (APTES, 99%) was purchased from Sigma-Aldrich. Borosilicate

glass slides (22 mm × 22 mm, thickness 0.1–1.0 mm) were purchased from HmbG. Alginic acid (Sigma-Aldrich), chitosan (Sigma-Aldrich) and starch (Chemical Reagents, China National Chemical Import and Export Corporation Peking Branch) were used as the biopolymer surfactants. All the reagents were of analytical grade in purity and used without any further purification. Ultrapure water (~18.2 MΩ cm⁻¹, 25°C) was used in all synthesis processes.

2.2 Preparation of APTES Functionalised Glass Slides

Glass slides were functionalised with APTES for the coating of ZnS NPs based on the method reported by Lim et al.²⁰ First, the glass slides were cleaned with the piranha solution, which was a mixture of sulphuric acid and hydrogen peroxide with the ratio of 3:1. They were immersed into the solution for 1 h and next rinsed with ultra-pure water (UPW). The cleaned glass slides were air-dried prior to immersion in 10% v/v APTES in absolute ethanol for 2 h for amine functionalisation via the silanisation process. Then, they were rinsed with absolute ethanol to remove any excess APTES on the glass slides surfaces, followed by heat treatment at 120°C for 30 min.

2.3 Sample Preparation

2.3.1 Synthesis of ZnS NPs suspension

ZnS NPs were synthesised based on the method reported by Shahi et al., with some modifications.¹³ An amount of 0.55 g zinc acetate dihydrate was added into the 50 ml of UPW and stirred continuously until a homogeneous solution was obtained. Subsequently, 0.19 g of thiourea was added to the solution, which was then kept under vigorous stirring for 2 h.

The chemical process can be described using the following chemical reactions:



Overall reactions:



2.3.2 Synthesis of ZnS NPs suspension with surfactant

The synthesis method was similar to synthesising ZnS NPs as detailed in Section 2.3.1, except for the addition of starch, alginic acid and chitosan were added into the ZnS suspension as the surfactants. First, zinc acetate dihydrate was added into 50 ml of UPW water. Then, 0.19 g of thiourea was added to the mixture under stirring, whereby the solution was continuously stirred for the following 2 h. An amount of 0.05 g of the biopolymer (i.e., starch, alginic acid and chitosan) was next added into the solution which altered the concentration of the surfactant to 0.1% w/v. The solution was stirred for 24 h for the solution achieving its equilibrium.



2.3.3 Deposition of ZnS nanocrystalline thin film

The ZnS nanocrystalline thin film deposition was carried out by the spin-coating technique using a spin coater (GLICHN Technology T-108 Spin Coater). Small drops of ZnS NPs suspension were dropped on the centre of the APTES functionalised glass slides by using a dropper, spun for 30 s at 1000 rpm and then heated at 90°C after each deposition. This process was repeated until five layers of thin films were deposited on the glass slides. Subsequently, the deposited thin films were annealed in a digital muffle furnace (WiseTherm FH Daihan 1200°C) at 300°C for 2 h to remove any volatile by-products and improve the crystallinity of the thin films. The annealed thin films were next rinsed with deionised water to remove any impurities on the thin film surface and dried in a desiccator until their further use for characterisation process.

2.4 Characterisation of ZnS Nanocrystalline Thin Film

Field emission scanning electron microscope (FESEM) images of the thin films were obtained using a FESEM model ZEISS Supra 55VP and energy dispersive X-ray (EDX). X-Ray diffraction (XRD) patterns of the films were produced using an X-ray diffractometer (Model Bruker D8 Advance) via monochromated CuK α radiation operated at 40 kV. The optical properties were studied using

a photoluminescence (PL) spectrometer (model Perkin Elmer LS 55) and an ultraviolet-visible (UV-Vis) spectrophotometer (model Lambda 650, Perkin Elmer).

3. RESULTS AND DISCUSSION

3.1 FESEM Analysis

Figure 1(a) shows the FESEM outcomes of the ZnS thin film without the addition of surfactants for a comparison with ZnS thin films that were capped with surfactants. The FESEM images revealed that the ZnS thin film (without surfactant) was composed of spherical nanoparticle size with mean particle sizes ranging from 27 nm to 36 nm, which were deposited uniformly throughout the glass slides. Figures 1(b–d) exhibit the FESEM images of biopolymers-capped ZnS thin films. The particle sizes range for all the samples are presented in Table 1. The particle size range of alginate-capped ZnS thin film was within the range of 16 nm to 23 nm, which was slightly smaller as compared to a ZnS thin film that lacked surfactant. This is due to the addition of biopolymer as the surfactants, which has greatly limited the growth of the nanoparticles and thereby resulting in smaller and more uniform mean particles sizes.¹⁹ The largest particles sizes within the range of 20–32 nm were obtained when chitosan was used as the surfactant. The larger particles sizes of ZnS as compared to ZnS without surfactant might be attributable to the large molecular weight of chitosan ($MW \sim 50,000 \text{ g mol}^{-1}$ to $190,000 \text{ g mol}^{-1}$). In contrast, the smallest particles sizes were obtained when starch was used as the surfactant and ranged between 9 nm and 20 nm as can be seen in Figure 1(d). This could be due to the highly viscous nature of the starch solution that could effectively limited the nucleation and growth of the nanoparticles.

Figure 2 shows the FESEM cross-sectional images and thin film thickness of: ZnS thin film without surfactant; alginate-capped ZnS thin film; chitosan-capped ZnS thin film; and starch-capped thin film. The thickness of the ZnS thin films without surfactant (223 nm) and the thin films capped with alginate (228 nm) is about the same. Even though the particle sizes of the thin films without surfactant are larger, the coating of alginate has added to the thickness of the thin films. From Figure 2(b), it also can be observed that the addition of alginate as the surfactant improved the adherence of ZnS NPs on the surface of the glass slides, and that the thin film was well-assembled. This might be due to the characteristics of alginate itself as a good binding agent, viscosifier, and stabilising agent.²¹ Its ability of alginate as a binder gave rise to the closely packed ZnS nanocrystalline thin film. Meanwhile, Figure 2(c) shows that the thickness of the

chitosan-capped ZnS thin film of 536 nm which was thicker as compared to ZnS, alginate-capped ZnS, and starch-capped ZnS thin film. This can be explained by the larger particles size of ZnS NPs that have resulted in an increased thickness of the thin film. As can be seen in Figure 2(d), the average thickness for starch-capped ZnS thin film was observed to be merely 109 nm. The decrease in the thin film thickness was due to the smaller particle sizes of starch-capped ZnS NPs.

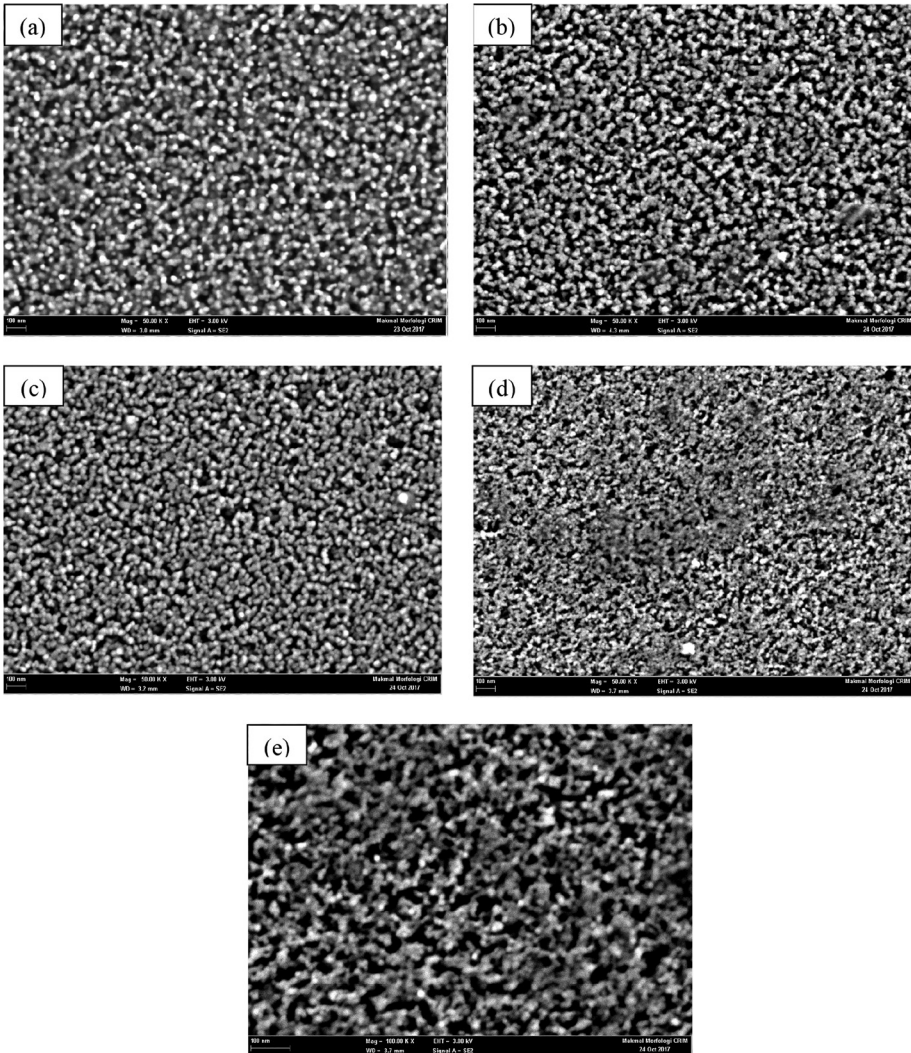


Figure 1: FESEM images of ZnS films with 50,000X magnification for (a) ZnS without surfactants, (b) alginate acid-capped ZnS, (c) chitosan-capped ZnS, (d) starch-capped ZnS nanocrystalline thin film, and (e) starch-capped ZnS nanocrystalline with 100,000X magnification.

Table 1: Average ZnS nanoparticle size and thin films thickness.

Sample	Average nanoparticles size (nm)	Thin film thickness (nm)	Band gap (eV)
ZnS	27–35	223	4.85
Alginate acid-capped ZnS	16–23	228	4.83
Chitosan-capped ZnS	20–32	369	4.85
Starch-capped ZnS	9–21	110	4.75

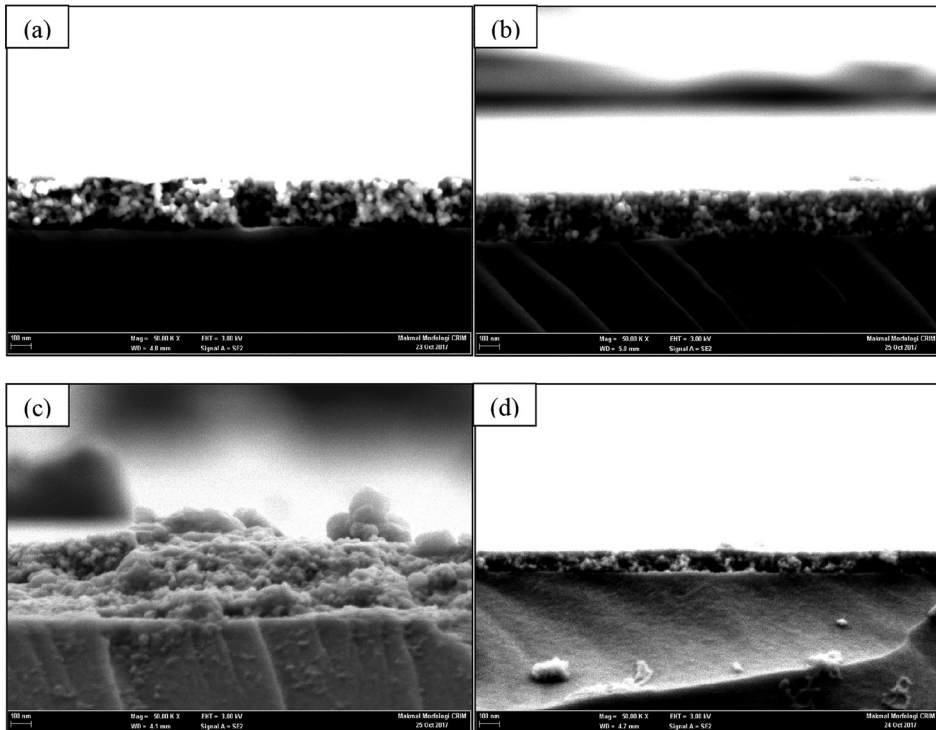


Figure 2: FESEM cross sectional images with 50,000X magnification of (a) ZnS thin film without surfactant, (b) alginate acid-capped ZnS thin film, (c) chitosan-capped ZnS thin film, and (d) starch-capped ZnS thin film.

3.2 XRD

The XRD patterns of the ZnS thin films are presented in Figure 3. The broad hump observed within the range $2\theta = 15^\circ\text{--}40^\circ$ was due to the amorphous glass substrate. The spectra exhibited three peaks at about 29° , 47° and 57° which were corresponding to the (111), (220), and (311) crystal planes of the cubic ZnS phase.^{23,24}

The average size (D) was calculated using the Debye-Scherrer formula as follows:

$$D = \frac{0.9\lambda}{\beta \cos \theta}$$

where λ is the wavelength ($\text{CuK}\alpha$, radiation equals to 1.5406 nm), θ is the Bragg diffraction angle and β is the Full Width at Half Maximum (FWHM) of the XRD peak appearing at the diffraction angle θ .

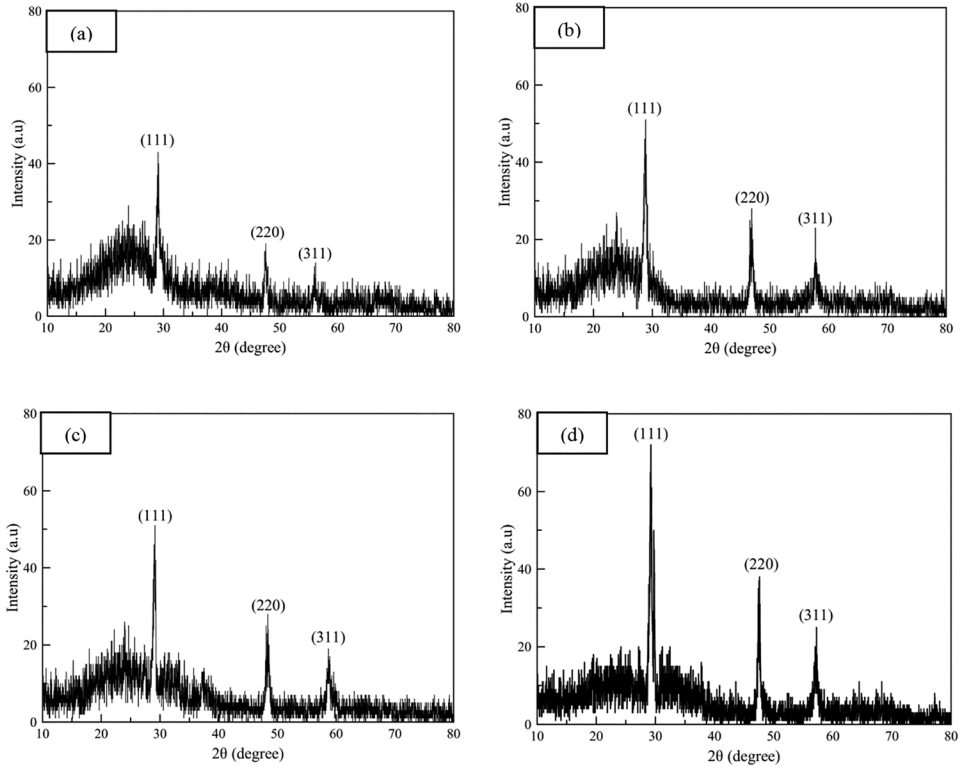


Figure 3: XRD diffractograms of (a) ZnS without surfactants; and ZnS films capped with various types of biopolymer surfactants, i.e., (b) alginate, (c) chitosan, and (d) starch.

Figure 3(a) shows that the ZnS thin film without the presence of surfactant exhibited weaker diffraction peak, which is indicative of the film's low degree of crystallinity. Meanwhile, all the thin films capped with biopolymer surfactants displayed stronger diffraction peak intensity, suggesting their higher degree of crystallinity.²² The results obtained from the XRD analysis are summarised in Table 2. The average crystallite sizes of ZnS nanocrystalline thin films

were calculated using the Debye-Scherrer equation and varied from 1.71 nm to 2.98 nm. To reduce error, only the crystallite size for peak (111) of each surfactant-capped thin film was calculated. From the calculations, it can be concluded that the estimated crystallite size of ZnS NPs decreases with the addition of various biopolymers surfactants. It is found that alginic acid, chitosan and starch-capped ZnS thin film yielded an estimated crystallite size of 2.63 nm, 2.76 nm and 1.71 nm, respectively. In contrast, ZnS thin film without a surfactant obtained an estimated crystallite size of 2.98 nm, which was larger than their surfactant-capped counterparts.

Table 2: Results from the XRD of ZnS thin films with various types of surfactants.

Samples	Intensity	2θ (degree)	FWHM (degree)	hkl	d_{hkl}	Avg. a (Å)	Crystallite size (D)
ZnS	43	29.06	0.48	(111)	3.17	4.86	2.98
	19	47.64	0.58	(220)	1.91		
	13	56.02	1.36	(311)	1.64		
Alginic acid- capped ZnS	51	28.86	0.54	(111)	3.09	4.83	2.65
	28	46.92	0.56	(220)	1.93		
	23	57.76	0.44	(311)	1.59		
Chitosan-capped ZnS	51	29.14	0.52	(111)	3.06	4.76	2.76
	25	48.06	0.46	(220)	1.89		
	17	58.66	1.32	(311)	1.57		
Starch-capped ZnS	64	29.14	0.84	(111)	3.06	4.82	1.71
	35	47.42	0.36	(220)	1.92		
	25	57.02	0.62	(311)	1.61		

3.3 UV-Vis Analysis

Figure 4 shows the UV-Vis absorption spectra of the ZnS thin films that are capped with various biopolymer surfactants. All ZnS thin films showed excitation peaks at approximately at 250 nm which was in agreement with Noor et al.'s observation for ZnS having a great potential to absorb light at a wavelength ranging between 220 nm and 350 nm.⁹

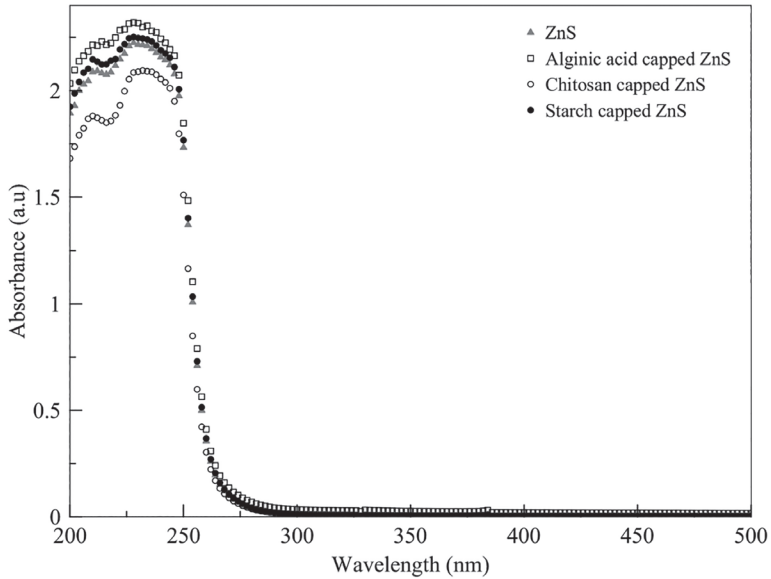


Figure 4: UV-Vis absorption spectra of ZnS thin films and ZnS thin films capped with various types of biopolymer surfactants.

Figure 5 shows the optical transmission of the ZnS thin films that ranged between 200 nm and 800 nm as derived from Beer's law equation as shown below, where A = absorbance, and T = transmittance.

$$A = \log_{10}\left(\frac{1}{T}\right)$$

$$A = -\log_{10}(T)$$

$$T = 10^{(-A)}$$

$$\%T = T(100)$$

$$\%T = 100(10^{(-A)})$$

The films deposited shows transmittance values of 99%, 92%, 97% and 97% for ZnS thin film without surfactant, alginic acid-capped ZnS, chitosan-capped ZnS and starch-capped ZnS thin films, respectively. The deposited ZnS thin films deposited exhibit a high optical transmission and anti-reflector properties that may be suitable to be used as anti-reflective materials.³

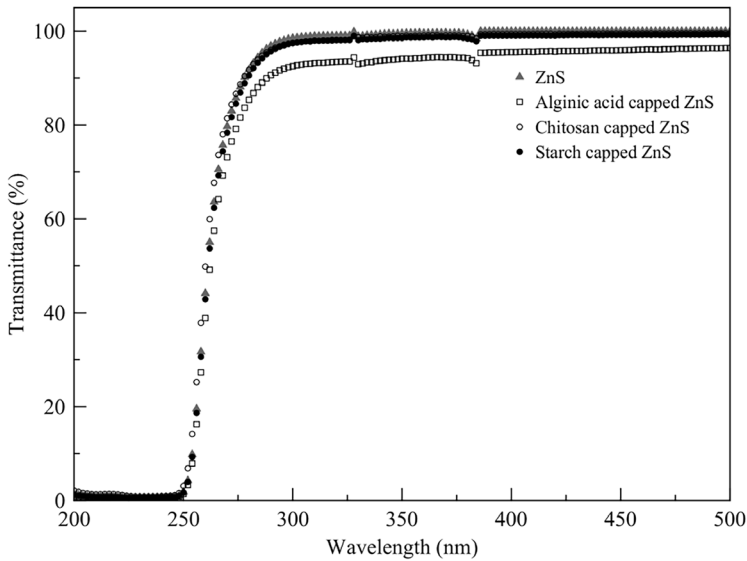


Figure 5: Transmittance spectra of ZnS nanocrystalline thin films capped with various types of biopolymer surfactants.

Figure 6 exhibits the band gap energy values (E_g) of various surfactant-capped ZnS thin films obtained by the UV-Vis spectrophotometer. Since ZnS is a semiconductor material with a direct band gap, the E_g value can be determined by using the Tauc's formula. The E_g value of the films can be evaluated by extrapolating the straight portion to the $h\nu$ based on the equation below:

$$(\alpha h\nu)^2 = A(h\nu - E_g)^m$$

where α is the adsorption coefficient, $h\nu$ is the photon energy (eV), A is the energy independent constant, E_g is the band gap value and m is the constant that determines the type of optical transmission ($m = 2$ for indirect, $m = 1/2$ for direct transmission). Meanwhile, the adsorption coefficient can be calculated from the transmission spectrum using the following equation:

$$\alpha = \frac{1}{d \ln\left(\frac{1}{T}\right)}$$

where d is the thin film thickness and T is the percentage transmission.

The band gap value of ZnS films without surfactant was observed to be higher (4.85 eV) than its reported band gap value of 3.8 eV. The observation was related to the quantum confinement effects caused by the small-grain size of ZnS NPs

synthesised in this study.²⁵ Based on Figure 6, the band gap value is not dependent upon the quantum size or the film thickness. This may be correlated with the types of surfactant added, whereby different types of surfactants have given rise to different band gap values. When alginic acid was used as the surfactant, the band gap value obtained was 4.83 eV, whereas, the use of chitosan as the surfactant yielded a band gap value of 4.85 eV. Meanwhile, starch-capped ZnS thin film generated the band gap value of 4.75 eV.

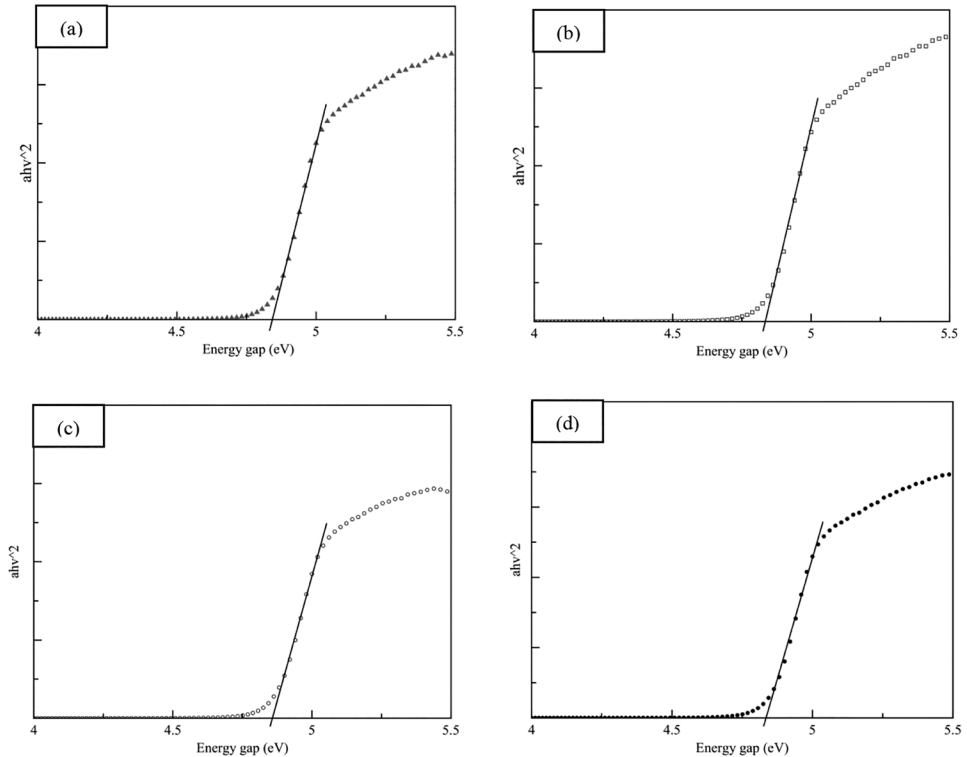


Figure 6: Tauc's plots, i.e., plots of $(\alpha h\nu)^2$ vs. $h\nu$ for (a) ZnS (without surfactants), (b) alginic acid capped ZnS thin film, (c) chitosan capped ZnS thin film, and (d) starch capped ZnS thin films.

3.4 Photoluminescence Analysis

Figure 7 illustrates the room temperature photoluminescence (PL) spectra of all the ZnS thin films, which were recorded at 300 nm excitation wavelength. The PL spectra consequently displayed very wide bands ranging between 350 nm and 700 nm. All the ZnS thin films exhibited the same pattern broad peaks centred at around 470 nm, 620 nm and 690 nm but each showed different emission intensity.

The first peak shows that the films are in the blue shift, which is attributable to the zinc vacancies seen at the valence band, while second excitation occurs at the second peak that is not related to the samples, as it could be sourced from the glass slides.²⁶ The last peak shows the recombination process that is dependent on the quality of the prepared sample (sample purity), electronic band structure and the properties of the band gap.

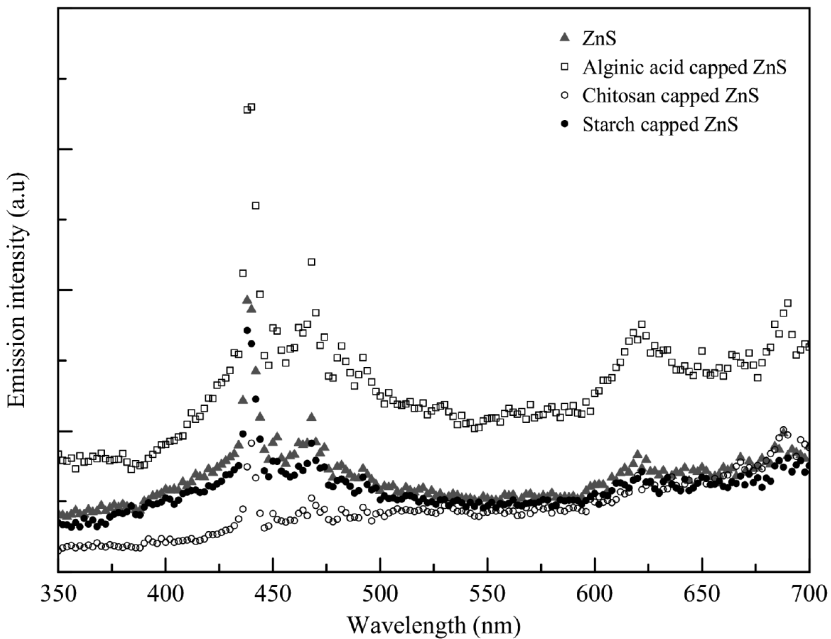


Figure 7: PL spectra of (a) ZnS thin film without surfactant, (b) alginic acid-capped ZnS thin film, (c) chitosan-capped ZnS thin film, and (d) starch-capped ZnS thin films at a 350 nm excitation wavelength.

4. CONCLUSION

Various biopolymers-capped ZnS nanocrystalline thin films were successfully prepared by the combination of sol-gel and spin coating techniques. XRD patterns confirmed the cubic crystalline structure of ZnS NPs. The morphology of the thin films was identified using the FESEM analysis, revealing a spherical-shaped nanoparticulate with an average size and thickness that ranged between 20–30 nm and 109–536 nm, respectively. Furthermore, the optical characterisation (UV-Vis absorption) revealed that the band gap of ZnS nanoparticulate thin films were 4.85 eV, 4.83 eV, 4.85 eV and 4.78 eV for ZnS without surfactant and ZnS capped with alginic acid, chitosan and starch, respectively. Meanwhile, the PL

spectra showed broad peaks at approximately 470 nm and 620 nm. Various types of biopolymer surfactants were observed to be capable of stabilising and impacting the particle sizes of ZnS NPs as well as indirectly controlling the thickness of the thin films. In conclusion, starch-capped ZnS NPs thin film yielded the best morphological properties, whereby in comparison with the ZnS thin film without surfactant and other surfactant-capped ZnS thin films, its nanoparticles and the thin film were more controlled.

5. ACKNOWLEDGEMENTS

The financial support by the Ministry of Education (MOE) through the Research Acculturation Grant Scheme RAGS/SG01(1)/1310/2015(04) is gratefully acknowledged. Special thanks to the Faculty of Resource Science and Technology for the analysis work and the Physics Laboratory of the Centre of Pre-University Studies, Universiti Malaysia Sarawak for the laboratory works.

6. REFERENCES

1. Farid, H. et al. (2014). Preparation and characterization of ZnS nanocrystalline thin films by low cost dip technique. *J. Mater. Sci. Mater. Electron.*, 25(5), 2017–2023, <https://doi.org/10.1007/s10854-014-1790-9>.
2. Kavanagh, Y. & Cameron, D. C. (2001). Zinc sulfide thin films produced by sulfidation of sol-gel deposited zinc oxide. *Thin Solid Films*, 398, 24–28. [https://doi.org/10.1016/S0040-6090\(01\)01298-6](https://doi.org/10.1016/S0040-6090(01)01298-6).
3. Ofor, P. O. et al. (2015). Synthesis and characterization of nanocrystalline zinc sulphide thin films by chemical spray pyrolysis. *J. Alloy Comp.*, 650, 381–385, <https://doi.org/10.1016/j.jallcom.2015.07.169>.
4. Goktas, A. et al. (2012). Preparation and characterisation of thickness dependent nano-structured ZnS thin films by sol-gel technique. *J. Mater. Sci. Mater. Electron.*, 23(7), 1361–1366, <https://doi.org/10.1007/s10854-011-0599-z>.
5. Shanmugam, N. et al. (2013). Effect of annealing on the ZnS nanocrystals prepared by chemical precipitation method. *J. Nanomater.*, Article ID 351798, <https://doi.org/10.1155/2013/351798>.
6. Ravichandran, K. & Nedumaran, D. (2011). Synthesis and characterization of zinc sulfide nanoparticles using inert gas condensation technique. *Int. J. Mech. Eng. Mater. Sci.*, 4, 25–31.
7. Xu, J. F. et al. (1998). Preparation of ZnS nanoparticles by ultrasonic radiation method. *Appl. Phys. A*, 66(6), 639–641, <https://doi.org/10.1007/s003390050725>.
8. Liu, J. et al. (2009). Synthesis of ZnS nanoparticles via hydrothermal process assisted by microemulsion technique. *J. Alloy Comp.*, 486(1–2), L40–L43, <https://doi.org/10.1016/j.jallcom.2009.07.109>.

9. Noor, A. A. et al. (2017). Effect of annealing temperature and spin coating speed on Mn-doped ZnS nanocrystals thin film by spin coating. *J. Nanomater.*, Article ID 2560436, <https://doi.org/10.1155/2017/2560436>.
10. Stefan, M. et al. (2013). Synthesis of luminescent zinc sulphide thin films by chemical bath deposition. *J. Alloy Comp.*, 548, 166–172, <https://doi.org/10.1016/j.jallcom.2012.09.013>.
11. Brahma, S. et al. (2015). Effect of substrates and surfactants over the evolution of crystallographic texture of nanostructured ZnO thin films deposited through microwave irradiation. *Thin Solid Films*, 593, 81–90, <https://doi.org/10.1016/j.tsf.2015.09.005>.
12. Charinpanitkul, T. et al. (2005). Effects of cosurfactant on ZnS nanoparticle synthesis in microemulsion. *Sci. Technol. Adv. Mater.*, 6(3–4), 266–271, <https://doi.org/10.1016/j.stam.2005.02.005>.
13. Shahi, A. K. et al. (2011). Surfactant assisted surface studies of zinc sulfide nanoparticles. *Appl. Surf. Sci.*, 257(23), 9846–9851, <https://doi.org/10.1016/j.apsusc.2011.06.046>.
14. Pawar, N. B. et al. (2012). Effect of surfactant on optical and structural properties of chemically deposited MoBi₂S₅ thin films. *New J. Chem.*, 36(9), 1807–1812, <https://doi.org/10.1039/c2nj40341b>.
15. Dhanam, M. et al. (2009). Analysis of ZnS nanoparticles prepared by surfactant micelle-template inducing reaction. *Chal. Lett.*, 6(12), 713–722.
16. Mehta, S. K. et al. (2009). Effect of cationic surfactant head groups on synthesis, growth and agglomeration behavior of ZnS nanoparticles. *Nanosc. Res. Lett.*, 4(10), 1197, <https://doi.org/10.1007/s11671-009-9377-8>.
17. Ayodhya, D. et al. (2013). Synthesis, characterization of ZnS nanoparticles by coprecipitation method using various capping agents: Photocatalytic activity and kinetic study. *IOSR-JAC*, 6(1), 101–109, <https://doi.org/10.9790/5736-0610109>.
18. Senapati, U. S. & Sarkar, D. (2015). Synthesis and characterization of biopolymer protected zinc sulphide nanoparticles. *Superlatt. Microstr.*, 85, 722–733, <https://doi.org/10.1016/j.spmi.2015.06.040>.
19. Sreejith, L., Nair, S. M. & George, J. (2010). Biopolymer surfactant interactions. In Elnashar, M. (ed), *Biopolymers*. London: InTech Open, 612. <https://doi.org/10.5772/10272>.
20. Lim, L. S. et al. (2017). A novel silver nanoparticles-based sensing probe for the detection of Japanese Encephalitis virus antigen. *Sains Malays.*, 46(12), 2447–2454, <https://doi.org/10.17576/jsm-2017-4612-21>.
21. Donati, I. & Paoletti, S. (2009). Material properties of alginates. In Rehm, B. H. A. (ed.), *Alginates: Biology and applications*. Berlin: Springer, 1–53. https://doi.org/10.1007/978-3-540-92679-5_1.
22. Al-khayatt, A. H. O. & Jaafer, M. D. (2014). Characteristics of nanocrystalline ZnS thin films grown on glass with different Zn ion concentrations by CBD technique. *J. Appl. Phys.*, 6, 27–35, <https://doi.org/10.9790/4861-06132735>.
23. Zein, R. & Alghoraibi, I. (2014). Effect of deposition time on structural and optical properties of ZnS nanoparticles thin films prepared by CBD method. *Int. J. Chemtech. Res.*, 6(5), 3220–3227.

24. Chen, H. & Gui, L. (2015). Preparation of ZnS modified PHBV Film by chemical bath deposition method. *Proceed. Int. Conf. Chem. Mater. Food Eng.*, 3–6, <https://doi.org/10.2991/cmfe-15.2015.1>.
25. Sartale, S. D. et al. (2005). Preparation of nanocrystalline ZnS by a new chemical bath deposition route. *Thin Solid Films*, 480, 168–172, <https://doi.org/10.1016/j.tsf.2004.11.054>.
26. Denzler, D., Olschewski, M. & Sattler, K. (1998). Luminescence studies of localized gap states in colloidal ZnS nanocrystals. *J. Appl. Phys.*, 84(5), 2841–2845, <https://doi.org/10.1063/1.368425>.